

CC

JET-P(95)39


The JET Team  
presented by T T C Jones

---

---

# The Route to High Performance on JET

CERN LIBRARIES, GENEVA  
SCAN-9510103



SW 9542

---

JOINT EUROPEAN TORUS

**JET**

This document is intended for publication in the open literature. It is made available on the understanding that it may not be further circulated and extracts or references may not be published prior to publication of the original, without the consent of the Publications Officer, JET Joint Undertaking, Abingdon, Oxon, OX14 3EA, UK.

Enquiries about Copyright and reproduction should be addressed to the Publications Officer, JET Joint Undertaking, Abingdon, Oxon, OX14 3EA, UK.

# The Route to High Performance on JET

The JET Team  
presented by T T C Jones

JET Joint Undertaking, Abingdon, Oxfordshire, OX14 3EA, UK.

Preprint of an Invited paper submitted for publication in a  
special issue of Controlled Fusion and Plasma Physics

August 1995



# The Route to High Performance on JET

The JET Team<sup>1</sup>  
(presented by T T C Jones)

JET Joint Undertaking, Abingdon, Oxfordshire, OX14 3EA, UK

**Abstract.** The capability of the Mk. I JET pumped divertor to give access to high performance plasma regimes has been successfully demonstrated. The considerable flexibility afforded by the divertor coil configuration and plasma position control system, together with operation of the torus cryo-pump, have facilitated a very extensive programme of experiments to determine optimum scenarios for maximising the total neutron emission from D-D reactions, fusion product  $n_D(0)\tau_E T_i(0)$  and equivalent  $Q_{DT}$ . Progress towards sustainable steady-state conditions at high fusion performance is also discussed.

## 1. Introduction

A substantial part of the JET experimental programme conducted following the installation of the Mk I pumped divertor (JET-PD) [1] has been devoted to establishing plasmas with high fusion performance characteristics. The overall aims of this high performance campaign can be summarised as follows.

i) To create conditions in deuterium plasmas which would correspond to high fusion power output in similar 50:50 deuterium-tritium plasmas, i.e.  $Q_{DT}^{equiv} \approx 1$  maintained for a time  $t \geq \tau_E$ , thus allowing an examination of  $\alpha$ -particle heating effects in future DT experiments.

ii) To establish the highest value of  $Q_{DT}^{equiv}$  compatible with reactor-like plasma conditions, especially in terms of high density and equilibrated ion and electron temperatures, sustained in steady-state. This would permit an eventual study of specific DT physics issues pertaining to a reacting divertor tokamak plasma, e.g. confinement, H-mode threshold, RF heating schemes, etc.

The above broad experimental areas will form the basis of a limited DT campaign in JET ('DTE1') planned to take place towards the end of the 1996 experimental programme.

The general characteristics of the hot-ion H-mode regime are discussed in section 2. This regime gives access to the highest fusion reactivity and fusion amplification factor  $Q$ , and was exploited for the JET preliminary tritium experiment [2], carried out in the previous JET machine configuration. Section 3 discusses in detail the re-optimisation of the hot-ion H-mode in the JET-PD, exploiting the new features such as active cryo-pumping and the capability of the plasma shape and position control system to provide favourable single-null X-point configurations over a wide range of plasma current. Experiments aimed at developing high performance scenarios which are sustainable towards steady-state operation have been carried

---

<sup>1</sup> See Appendix I of Reference [19]

out; the significant progress in this direction is described in section 4. A summary of achieved fusion performance is presented in section 5, where the results are extrapolated to DT plasmas making use of a simple ratio method [3] for relating the DD and DT reaction-rates, as well as detailed predictions based on the TRANSP [4] code on selected discharges. Finally, prospects for future performance improvements are briefly discussed in section 6.

## 2. General characteristics of hot-ion H-mode

### 2.1 High $\tau_E$

'Hot-ion mode' describes a regime in which intense plasma heating by neutral beams (NB) at low electron density results in a situation where the electron temperature is raised sufficiently such that NB predominantly heats the ions [5], whilst simultaneously the heat exchange between ions and electrons is weak compared with conduction losses.

Under these circumstances  $T_i$  can exceed  $T_e$  over a considerable proportion of the plasma volume and the conduction losses are predominantly via the ion channel which is characterised by low thermal diffusivity. The centralised deposition of NB power associated with low target density is a further factor contributing to the favourable confinement properties, and the central fuelling helps to sustain a moderately peaked density profile. In the hot-ion H-mode the edge transport barrier causes substantial edge ion and electron temperatures to develop, giving rise to a large contribution to the total plasma thermal energy  $W_{\text{thermal}}$  from the associated 'pedestal energy'. These characteristic features are evident in the data shown in figure 1 which refers to a time point approximately 1 second after the start of high power NB heating in a hot-ion H-mode.

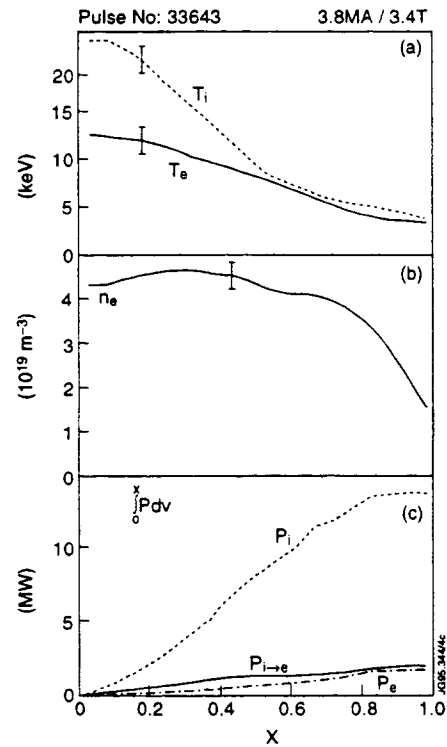


**Figure 1.** Profiles of (a) ion and electron temperature, (b) electron density (c) rate of heating and ion-electron energy exchange integrated over the volume within a given minor radius at the time of maximum stored energy in hot-ion H-mode discharge #33643

Figure 2 shows the time evolution of the components of the total plasma stored energy in the same discharge, in particular showing that  $W_{\text{pedestal}}$  contributes  $\approx \frac{1}{2} W_{\text{thermal}}$ , where:

$$W_{\text{pedestal}} = \frac{3}{2} \left[ T_i(a) \int_V n_i dV + T_e(a) \int_V n_e dV \right]$$

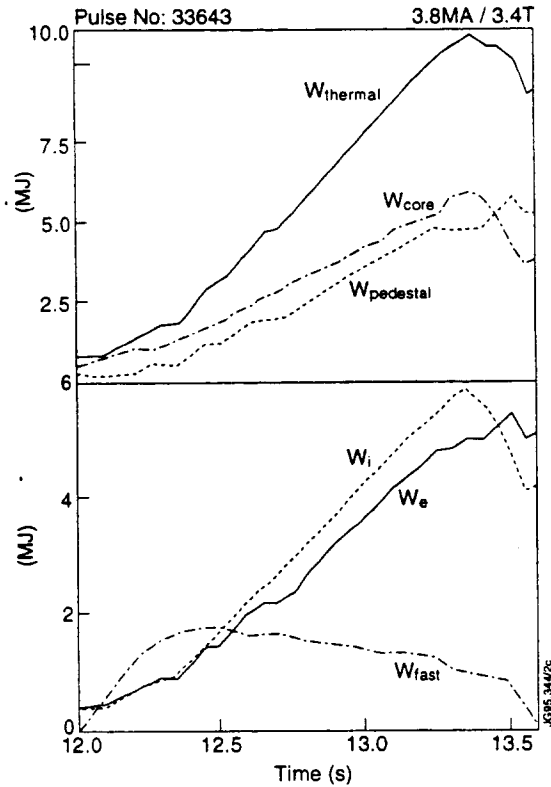


**Figure 2.** Contribution of different components to the plasma stored energy for pulse #33643

## 2.2 High reactivity and fusion $Q$

High fusion reactivity  $R$  per unit stored energy  $W$  results from the fact that  $T_i$  is above  $\approx 10\text{keV}$  over a significant fraction of the volume, in which temperature range the variation of the fusion reaction rate coefficients  $\langle\sigma v\rangle$  for DD and DT is such as to minimise the product  $n_i T_i$  for a given reaction rate. There is an additional gain in  $R/W$  because the dominant component of  $W$  is the ion thermal energy  $W_i$ , in consequence of the condition  $T_i > T_e$ . A significant contribution to the reactivity is also provided from the unthermalised beam ions responsible for the fast ion energy content  $W_{\text{fast}}$ . Thus the fusion  $Q$  value is maximised, since  $Q \propto \tau_E \cdot (R/W)$ .

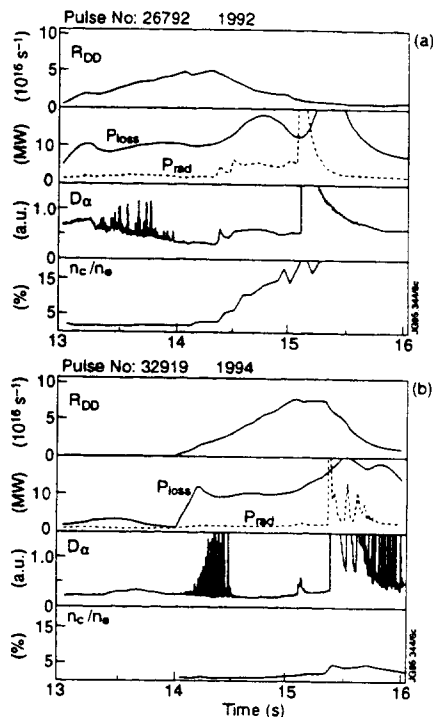
## 3. Optimisation of hot-ion H-mode for maximum performance

### 3.1 Consequences of operation with the Mk I pumped divertor machine configuration

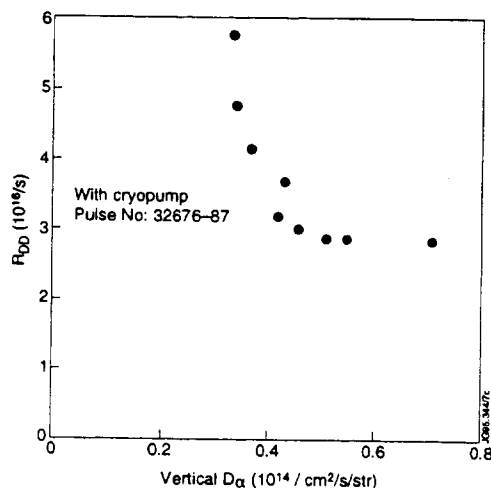
Optimised geometric design and accurate alignment tolerances of the divertor target tiles were expected to avoid the problem of impurity blooms resulting from overheated tile edges, in contrast to operation on the X-point dump plates of the previous JET configuration. This expectation was readily confirmed, and strong impurity blooms have been avoided. This is illustrated in figures 3a and b where a pair of similar discharges from the two campaigns are compared. Both exhibit onset of MHD activity and associated increase in loss power where  $P_{\text{loss}} = P_{\text{in}} - dW/dt$ ; in the older discharge a large influx of carbon was triggered whereas in the JET-PD discharge the carbon contamination, though increased, remains modest. It is thus possible to identify more clearly the influence of MHD stability upon performance, discussed in detail below, in contrast to results in the previous JET machine configuration in which these termination phenomena could not be clearly separated from the effects of blooms.

Active divertor cryo-pumping was extensively exploited with clear beneficial results. It has been shown [6] that high neutral pressures are developed at the entrance to the cryo-pump during ELMs which implies that there is a substantial particle removal rate under such

conditions. A cumulative reduction in particle recycling in successive discharges having periods of ELMs has been demonstrated, attributed to rapid conditioning of the divertor tiles.



**Figure 3.** Comparison of C impurity influx behaviour for a pair of similar high-performance discharges from (a) 1991-2 and (b) 1994-5 JET-PD campaigns



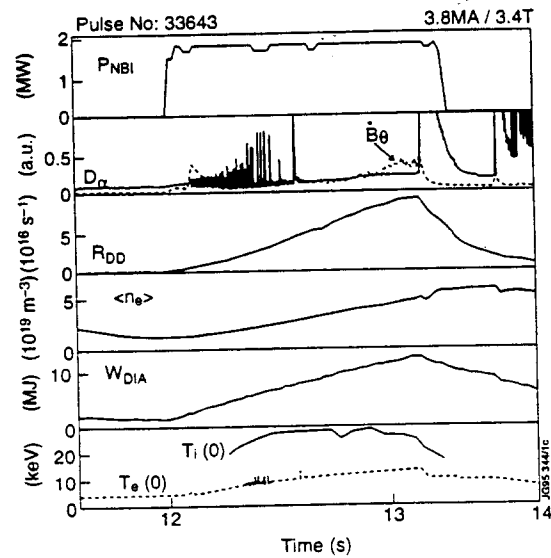
**Figure 4.** Shot to shot reduction in vertical  $D_{\alpha}$  intensity over successive discharges with active cryo-pumping, and improvement in DD reaction rate

Figure 4 shows the shot to shot reduction in  $D_{\alpha}$  intensity measured along a vertical chord over a series of consecutive hot-ion H-mode discharges at approximately similar power levels with the cryo-pump in operation, at the beginning of an experimental session. There is a strong influence on the maximum DD reaction rate as the  $D_{\alpha}$  intensity decreases, associated with successively increasing ELM-free duration and stored energy. A trend similar to that exhibited in figure 4 is evident when all the hot-ion H-mode data of the campaign are considered, although the interpretation is complex [7,8], due to the influence of other factors discussed later. It has been concluded that the main benefit of the cryo-pump in optimising performance results from cumulative particle removal and target depletion, rather than a direct influence of the pump during ELM-free periods when the measured neutral pressures are very low. Operation with the cryo-pump has facilitated access to vertical chord and main-chamber  $D_{\alpha}$  levels less than were otherwise achievable, including comparison with data from the previous JET campaign in 1991-2. From the discussion in section 1 it is evident that the hot-ion mode regime requires low target density and minimisation of the density rise during NB heating. The optimum target plasma formation technique involved maintaining an inner-wall limiter configuration until just before the start of NB heating in order to minimise the gas loading of the divertor target tiles. Apart from cases with very poorly conditioned target tiles, the volume integrated rate of density rise during ELM-free periods exceeded the beam-fuelled particle input by not more than about 30%. Even under the lowest prevailing recycling levels achieved with the cryo-pump, such as obtained in the discharge whose time evolution is shown in figure 5,



the density rise was never significantly less than the beam fuelling. The deleterious effects of particle recycling are therefore more subtle than a gross effect on density rise and beam deposition, and are described in detail in [7] where it is demonstrated, for example, that there is a link between low recycling and a prolongation of the duration of type III 'threshold' ELMs which may be beneficial in controlling the edge density and its gradient, and appear to delay the onset of edge MHD instabilities.

Other features of the 1994-5 machine configuration which potentially impact upon high performance operation include: reduction in plasma volume by  $\approx 20\%$  and a larger clearance from the conducting vessel wall; re-distribution of the available NB power between 80kV and 140kV D<sup>0</sup> beam sources to achieve a total power increase from 18 to 21MW, but weighted more towards the lower energy systems; slightly off-axis beam geometry in consequence of the up-down asymmetry of the JET-PD. The changes to the NB characteristics imply a larger fuelling rate for the same input power, which, combined with the volume reduction, results in a higher absolute rate of density rise.



**Figure 5.** Time evolution of the discharge giving rise to the highest recorded JET DD reaction rate

### 3.2 MHD termination events and their control

Hot-ion H-modes are subject to a variety of MHD events at high stored energy which cause the fusion performance to collapse, usually irreversibly. The discharge shown in figure 5, #33643 obtained in 1995, achieved JET's highest DD reaction rate,  $R_{DD} = 9.4 \times 10^{16} \text{ s}^{-1}$ , before final termination by a giant (type I) ELM and simultaneous sawtooth. This particular discharge was also subject to high frequency core ( $r \leq r_{q=1}$ ) MHD activity for  $\approx 200\text{ms}$  prior to the terminating ELM and sawtooth, which affects the central  $T_i$  value and rate of rise of  $R_{DD}$ , and is also picked up on the  $B_\theta$  coils. The effects of ELMs, occurring alone or in combination with core MHD events such as sawteeth, are discussed in detail in [9]. Another class of terminating MHD is characterised by a slow collapse of the plasma profiles and neutron emission, associated with low frequency ( $\approx 10\text{kHz}$ )  $n=1$ ,  $m \leq 5$  modes which are localised towards the outside of the plasma and have been tentatively identified as a saturated external kink [10]. These 'outer-modes' are also referred to as 'slow-rollovers' due to the characteristic effect on  $R_{DD}(t)$ . The MHD events which occur in both the discharges shown in figure 3 are of this type. Another example of this phenomenon is shown in detail in figure 6 which gives the evidence, confirmed by soft X-ray profiles [10], that the mode is localised towards the plasma edge. The data in figure 6 is from local  $T_e$  measurements derived from ECE emission; the initial increase in  $T_e$  is not understood and it is possible that an initial event triggers the mode activity indicated by the structure on the signal channels corresponding to the region  $r \geq r_{q=3}$ , observed simultaneously with increased levels of the  $D_\alpha$  and  $B_\theta$ -coil signals. Following the onset of the

outer-mode, a cold front propagates inwards across the entire profile. A statistical analysis of the abundance of the various classes of MHD termination events which affect high performance hot-ion modes, based on an examination of 141 discharges in which  $R_{DD} > 1 \times 10^{16} \text{ s}^{-1}$ , indicates that ELMs and outer-modes are involved in the majority of termination events.

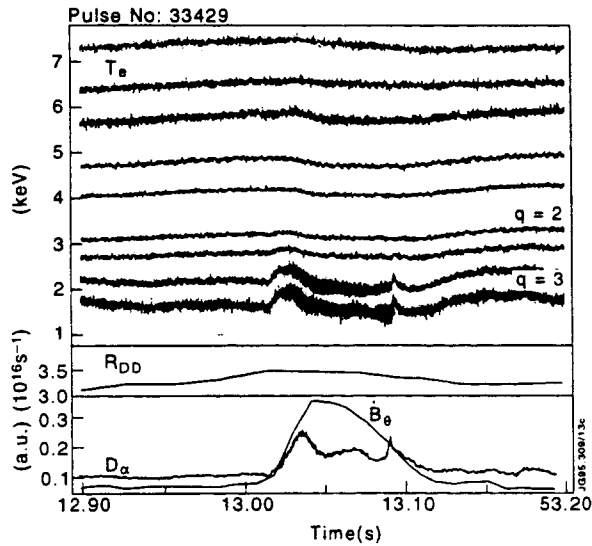


**Figure 6.** Spatial and temporal characteristics of 'outer-mode' or 'slow-rollover' event

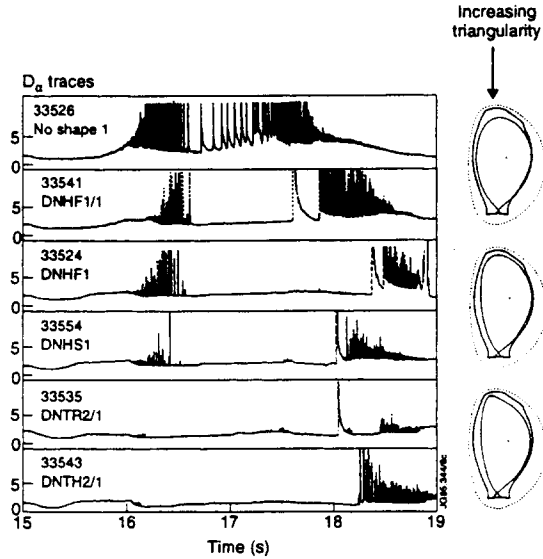


**Figure 7.** Comparison of ELM behaviour in plasma configurations of different shape. Triangularity and edge shear increase from top to bottom

**3.2.1 ELM control.** A strong link has been established between plasma shape and stability to ELMs, and hence performance. As discussed in section 3.1, recycling levels at the divertor target and main chamber walls were also observed to influence performance, at least partly due to the effect on ELM-free period. These various aspects of plasma behaviour are not independent of one another, which complicates the interpretation. The plasma configuration itself might be expected to influence main-chamber recycling due, for example, to variations in the degree of neutral leakage out of the divertor as the midplane-to-divertor flux-expansion ratio is varied. Code calculations [8] of the neutral particle dynamics indicate, however, that the main chamber recycling is largely insensitive to variation of flux-expansion for the configurations investigated experimentally. However, this result must be weighed against the observation in the experiments that there is a trend of increasing ELM-free period and lower recycling with increasing flux expansion [7]. A more direct link between plasma shape (in respect of triangularity, elongation and edge shear) and ELM-free period has been clearly established. Figure 7 shows the  $D_\alpha$  signatures of a number of moderate power ( $\approx 10\text{MW}$ ) H-modes for different plasma shapes. There is a clear qualitative difference in both the initial type III 'transition' ELMs and susceptibility to giant (type I) ELMs exhibited by the 'unshaped' discharge #33526 (shown first in sequence in figure 7), and the other configurations. The triangularity  $\delta$  and shear  $s$  at 95% of the minor radius vary in the range  $0.12 < \delta < 0.50$  and  $3.1 < s < 4.3$  respectively in figure 7. One of these configurations, #33524, was selected as the optimum for high-performance discharge development because it has the desired long

ELM-free period property and had the potential to be scaled to plasma current  $I_p > 4\text{MA}$  without exceeding the machine mechanical or power supply limits. The designation 'DNHF1' refers to the use of up-down symmetric shaping turns ratio, as used in previous double-null configurations, and the high flux-expansion characteristics of the configuration. It is interesting to note that the former double-null and single-null plasmas were naturally of high triangularity owing to the dominant contribution to the plasma shaping in those configurations from the leakage flux of the transformer magnetic circuit, arising when a controlled difference current is driven in the inner and outermost sets of coils. The typical value of triangularity in the 1991-2 campaign was  $\delta \approx 0.44$ , compared with  $\delta \approx 0.35$  for DNHF1. Comparison of the maximum figure of merit  $\beta\tau_E$  in the two campaigns with the DIII-D 'shape parameter'  $(I_a B q)^2 R / (1 + \kappa^2)$  shows a similar trend as that reported in [11], although there is insufficient variation of this parameter to establish a clear relationship in the 1994-5 data alone.

**3.2.2 Amelioration of outer-modes.** When the giant ELM is delayed by the use of the more highly shaped configurations, outer-modes often terminate the high performance phase. So far, it has not proved possible to eliminate the outer-modes by profile control techniques such as current ramps or application of LHCD; experiments on the latter in high-performance hot-ion H-modes did however demonstrate the ability to maintain  $q(0) > 1$  and eliminate sawteeth entirely [12]. The effect of the outer-mode was minimised by operation at high  $q$ ; this is illustrated in figure 8 which shows how the amplitude of the outer-mode signature on  $D_\alpha$  and the  $B_\theta$ -coils, as well as the severity of the  $R_{DD}$  'rollover', all decrease as the toroidal magnetic field  $B_T$  is increased.

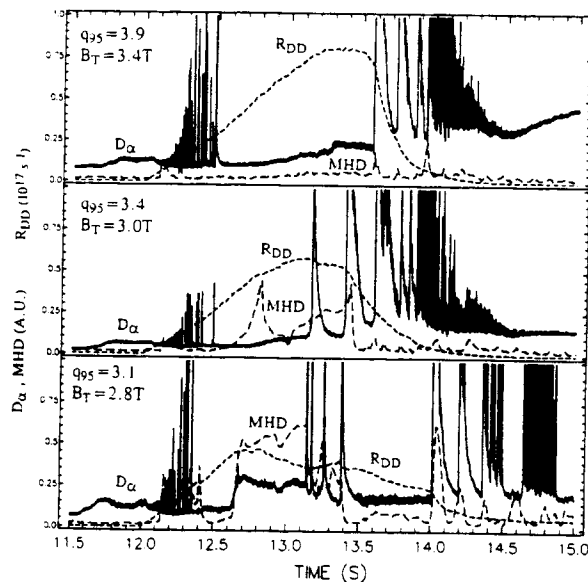


**Figure 8.** Effect of increasing  $q$  on severity of 'outer-mode' termination event

### 3.3 Confinement and beta limits at high performance

Confinement analysis of long ELM free hot-ion H-modes which are MHD quiescent shows that the global enhancement factor increases continuously until the termination. This is illustrated for three discharges in figure 9 where the thermal energy confinement time is normalised to the ITER93H-P ELM-free scaling prediction. Pulse #26087 is the discharge with the highest  $R_{DD}$  of the 1991-2 campaign which was classed as a VH mode owing to its high normalised confinement or H factor. Pulse #30591 is an early high-performance discharge in the 1994-5 campaign which is of only moderate fusion yield, and #33643 is the 1995 discharge with the highest  $R_{DD}$  in JET. A striking feature of the transport analysis of these three discharges is the

similarity of the effective thermal diffusivities over most of the plasma core, as shown in figure 10 and discussed in [13,14]. Therefore the differences in global confinement must be mainly governed by the evolution of the  $W_{\text{pedestal}}$  contribution, which is ultimately limited by the onset of MHD termination events, rather than by changes in the underlying core transport. It is not therefore surprising that there is considerable variation in the global confinement when normalised to a scaling law such as ITER93H-P; thermal H factors in the 1994-5 data range up to about 1.5 compared with 1.8 in 1991-2. Whilst the H factors for the recent campaign are lower, the important result is that similar absolute stored energies and slightly higher  $R_{\text{DD}}$  have been achieved by increasing the plasma current from 3 to 3.8MA and the heating power from 15 to 18.5 MW, comparing #26087 and #33643 respectively.

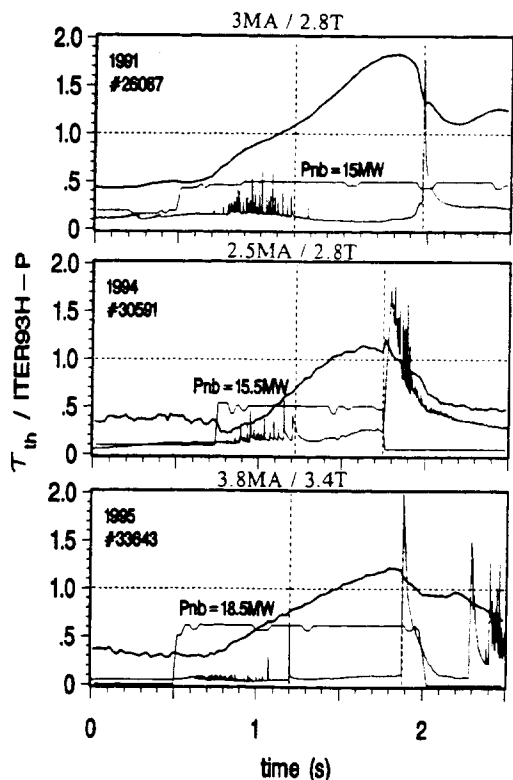


**Figure 9.** Time evolution of thermal energy confinement enhancement factors relative to ITER93H-P scaling law

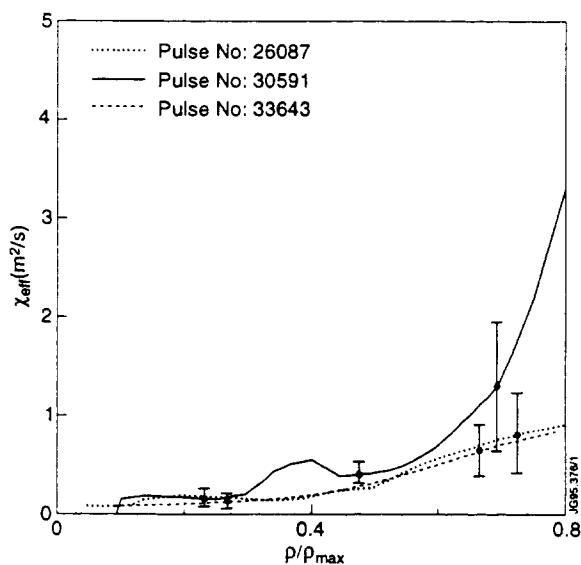


**Figure 10.** Effective single fluid thermal diffusivity for the same discharges shown in figure 9

Concerning the maximum normalised beta achieved in high performance plasmas, figure 11 shows that the discharges with the highest reactivity  $R_{\text{DD}}$  remain well below the Troyon limit. Other discharges at low plasma current can exceed the Troyon limit at high values of  $\beta_{\text{poloidal}}$  but these have low absolute stored energy and  $R_{\text{DD}}$ . This result implies that the pressure gradient is on average well below the ideal ballooning limit over the plasma profile. Stability calculations [9] confirm this is the case, except close to the plasma edge where the experimental values of  $\nabla p(a)$  approach  $\nabla p(\text{ideal ballooning})$ , as shown in figure 12 which demonstrates the advantage of raising  $I_{\text{p}}$  in respect of the achieved  $\nabla p(a)$  and therefore establishes a link between  $I_{\text{p}}$  and  $W_{\text{pedestal}}$ . It is concluded that while  $\nabla p(a)$  appears to be limited below the ideal ballooning limit, there is no evidence that ballooning modes are actually responsible for ELMs or outer modes; kink stability analysis [15] implies that the hot-ion H-mode discharges become kink unstable and MHD data suggest that terminating events do include an  $n=1$  kink.

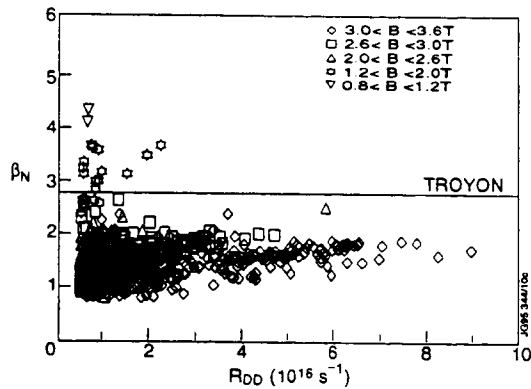


**Figure 11.** Relationship between normalised beta ( $\beta_N = \beta / (I_p / a B_T)$ ) and DD reaction rate for data from the 1994-5 campaign

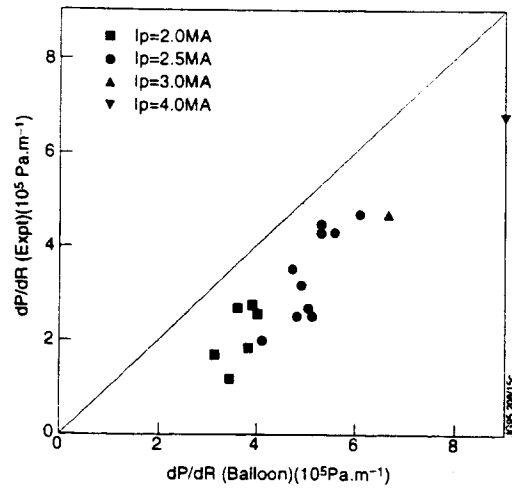


**Figure 12.** Maximum measured edge pressure gradients compared with the predictions of ideal ballooning theory

## 4. Progress towards high performance in steady-state conditions

### 4.1 Quasi-steady state hot-ion H-mode by power 'step-down'

It is possible to delay the termination of the high-performance phase by pre-programming a reduction in NB power in order to remain just below the MHD stability limit. In this way, high values of near-steady  $R_{DD}$  and diamagnetic stored energy  $W_{dia}$  have been maintained for up to 1s, with  $T_i$  and  $T_e$  beginning to converge [16]. Such a discharge is illustrated in figure 13; one important limitation of this technique is that the density continues to rise, although the rate of increase is reduced. In the discharge shown, following the step-down the density rise is minimised by retaining mostly the high voltage 140kV beams.

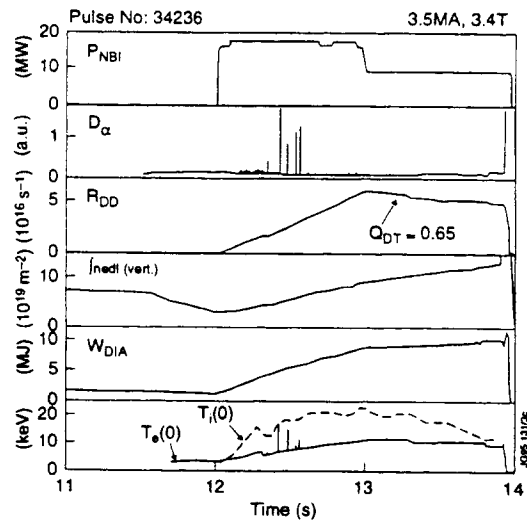


**Figure 13.** Time evolution of quasi steady-state power 'step-down' discharge #34236

### 4.2 Steady-state ELMy H-modes

ELMy H-mode conditions have been exploited to maintain near-steady conditions, including density; as mentioned in section 3.1 effective particle pumping is obtained during ELMs with the divertor cryo-pump in operation. By operating at high plasma current, favourable scaling of

$\tau_E$  with  $I_p$  in ELMy H-modes [17] has been exploited together with high power heating. Equilibrated ion and electron temperatures in the range 8-9 keV at  $\langle n_e \rangle \approx 6 \times 10^{19} \text{ m}^{-3}$  have been maintained for 1s using 20MW NB heating at 5MA. Higher parameters have been obtained using combined heating at up to 30MW, but the duration of the high power phase was not long enough to establish steady-state conditions.

## 5. Summary of achieved fusion performance

An estimate of the equivalent DT fusion power  $P_{DT}^{\text{equiv}}$  for a 50:50 DT plasma can be related to  $P_{DD}$  in a similar D plasma by the relationship  $P_{DT}^{\text{equiv}} = 210 \times P_{DD} \pm 5\%$  [3], valid under the assumption that the 140kV  $D^0$  beams are replaced with  $T^0$  at the same power and energy.  $P_{DT}^{\text{equiv}}$  thus estimated is plotted against total  $P_{\text{loss}}$  and also total input power  $P_{\text{in}}$  in figures 14a and 14b, where data for the two campaigns 1991-2 and 1994-5 are compared. The cases which are near steady-state are identified and the comparison of figures 14a and 14b serves to illustrate the effect of transient conditions in the definition of the fusion  $Q$  which is usually quoted relative to  $P_{\text{loss}}$  rather than  $P_{\text{in}}$ . The highest  $P_{DT}^{\text{equiv}}$  was pulse #33643 in the 1994-5 campaign, although  $Q_{DT}^{\text{equiv}}$  is slightly less than the best 1991-2 case because  $P_{\text{in}}$  and  $P_{\text{loss}}$  were higher.

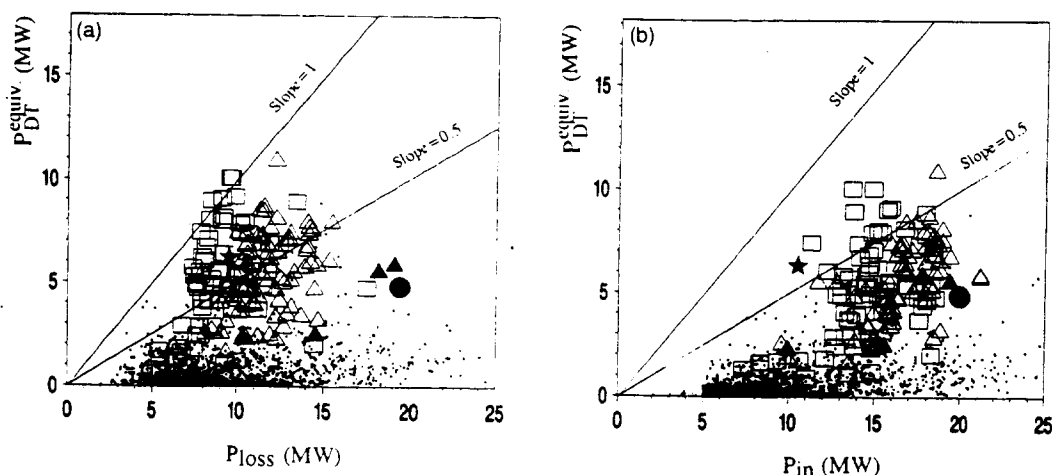


**Figure 14.**  $P_{DT}^{\text{equiv}}$  computed from the ratio method, compared with (a)  $P_{\text{loss}}$  and (b)  $P_{\text{in}}$ . Squares: 1991-2 data, Triangles: 1994-5 data ( large symbols satisfy  $T_i(0) > 1.5T_e(0)$ , solid symbols satisfy  $dW/dT < 0.1 P_{\text{in}}$ ). Filled star: 1995 quasi-steady 'stepdown' discharge. Filled circle: ELMy 5MA H-mode.

The plot of  $n_D(0)\tau_E T_i(0)$  versus  $T_i(0)$  is given in figure 15 which shows that the ranges of data in the two campaigns are similar and extend along a line characteristic of the hot-ion condition [18]; the highest value of  $n_D(0)\tau_E T_i(0)$  in 1994-5 is within 10% of the best 1991-2 data, consistent with the inferred  $Q_{DT}^{\text{equiv}}$  values in figure 14a.

Finally, TRANSP DT extrapolations have been carried out for discharge #33643 and the 'step-down' discharge #34236, under the assumption that the target plasma hydrogenic content is initially 50:50, and that the 7MW of 140kV  $D^0$  beams are replaced by  $T^0$  at the same power (however, the  $T^0$  power will actually be increased to 12.5MW in DTE1). The experimental plasma profiles are assumed in the calculations.

**Figure 15.** Fusion triple product plotted versus central ion temperature; Q contours are calculated referring to steady state conditions. Symbols as figure 14.

Figure 16a shows the comparison of the measured and predicted DD neutron emission for shot #33643 to validate the input data, together with the  $Q_{DT}^{equiv.}$  prediction. In figure 16b the predicted central electron heating by  $\alpha$ -particles is compared with the direct electron heating from NB, which indicates that a significant change to the electron power balance is expected, which would allow the investigation of  $\alpha$ -heating effects.

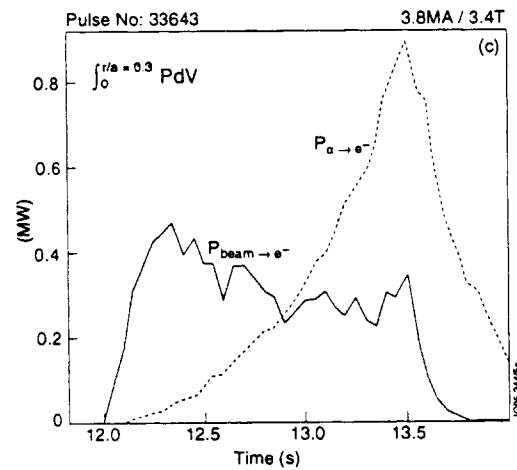
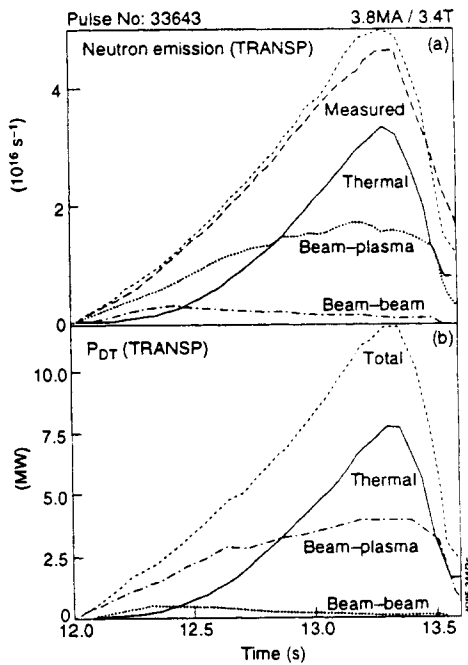
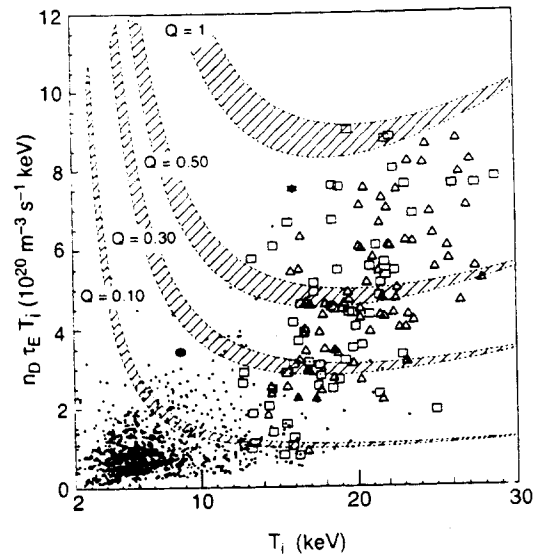


**Figure 16** (a) TRANSP prediction of (a) DD neutron emission and (b) projected DT power, and (c) comparison of central heating to electrons from  $\alpha$ -particles and direct beam heating from the DT TRANSP simulation of pulse #33643.

In the definition of  $Q_{DT}^{equiv.}$  used in [2], the component of  $\alpha$ -heating arising from thermal-thermal reactions is subtracted from  $P_{LOSS}$  in the denominator of the expression for the thermal-thermal contribution to  $Q_{DT}^{equiv.}$ , and NB shinethrough is discounted from the input power. On this basis the following results are obtained from the TRANSP extrapolations to DT:

- #33643: Max.  $Q_{DT}^{equiv.} = 1.07$  with  $Q_{DT}^{equiv.} > 0.7$  for 0.3s
- #34236: Max.  $Q_{DT}^{equiv.} = 0.82$  with  $Q_{DT}^{equiv.} > 0.7$  for 1.0s

## 6. Conclusions and prospects

Maximum fusion parameters have been obtained in JET-PD plasmas during 1994-5 similar to the best results from the previous 1991-2 campaign, in spite of the smaller plasma volume.  $Q_{DT}^{equiv} \approx 1$  has been obtained transiently, corresponding to predicted  $P_{DT}^{equiv} > 10$  MW.  $Q_{DT}^{equiv} > 0.7$  has been sustained for 1s at lower power, with  $P_{DT}^{equiv} \approx 6$  MW. The plasma conditions required for the planned DTE1 campaign in 1996 are therefore met. If MHD stability, especially at or near the plasma edge, and density control can be improved further, there are good prospects for even higher performance. A number of existing machine capabilities have not yet been fully exploited for high performance, i.e. LHCD profile control; ICRH for central heating without particle fuelling; active feedback control of the heating systems. In the next campaign, benefits are expected from the more closed Mk II divertor geometry in respect of recycling control. It is also proposed to increase the maximum  $B_T$  capability to 4T; in addition to the direct benefit expected from raising  $q$  this would also allow the present best scenarios to be scaled to  $I_p \approx 4.5$  MA at constant  $q$ , thus making better use of the high current capability of the machine.

## Acknowledgements

The work described here was mainly carried out by members of the JET High Performance Task Force and other JET Team members who are acknowledged gratefully and with pleasure by the author: P J Lomas, S Ali-Arshad, B Balet, M Bures, J P Christiansen, H P L de Esch, N Deliyakis, G Fishpool, T C Hender, G Huysmans, O N Jarvis, R König, K D Lawson, K M<sup>c</sup>Cormick, A C Maas, F B Marcus, M F Nave, R Sartori, B Schunke, P Smeulders, A Taroni, P R Thomas and K Thomsen.

## References

- [1] Bertolini E and the JET Team 1995 *Fusion Engineering and Design* **30** 53
- [2] The JET Team 1992 *Nuclear Fusion* **32** 187
- [3] Marcus F B *et al.* 1993 *Nuclear Fusion* **33** 1325
- [4] Goldston R J *et al.* 1981 *J. Comput. Phys.* **43** 61
- [5] Thompson E *et al.* 1993 *Phys. Fluids B* **7** 2468
- [6] Ehrenberg J *et al.* 1995 *Europhysics Conference Abstracts (Proc. 22<sup>nd</sup> European Conference on Controlled Fusion and Plasma Physics)*, EPS, Bournemouth, UK **Vol.19c (Part I)** 309
- [7] Lawson K D *et al.* 1995 *ibid (Part II)* 77
- [8] M<sup>c</sup>Cormick K *et al.* 1995 *ibid (Part I)* 313
- [9] Hender T C *et al.* 1995 *ibid (Part I)* 29
- [10] Smeulders P *et al.* 1995 *ibid (Part IV)* 61
- [11] Taylor T S *et al.* 1994 *Plasma Physics and Controlled Fusion* **36 Suppl.(12)** B229
- [12] Rimini F G *et al.* 1995 *Proc. 11<sup>th</sup> Topical Conference on RF Power in Plasmas, Palm Springs, USA*
- [13] Bak P *et al.* 1995 *Nuclear Fusion* (in press)
- [14] Erba M *et al.* 1995 *Europhysics Conference Abstracts (Proc. 22<sup>nd</sup> European Conference on Controlled Fusion and Plasma Physics)*, EPS, Bournemouth, UK **Vol.19c (Part II)** 213
- [15] Huysmans G *et al.* 1995 *ibid (Part I)* 201
- [16] Marcus F B *et al.* 1995 *ibid (Part II)* 53
- [17] Sartori R *et al.* 1995 *ibid (Part IV)* 141
- [18] Bickerton R J and the JET Team 1987 *Plasma Physics and Controlled Fusion* **29** 1219
- [19] Keilhacker M and the JET Team 1995 *Proc. 22<sup>nd</sup> European Conference on Controlled Fusion and Plasma Physics, EPS, Bournemouth, UK (Invited Paper) this volume*